Paleoanthropology

Evidence for a genetic disorder affecting tooth formation in the Garba IV child

Uri Zilberman[1], Patricia Smith[2], Silvana Condemi[3]

Introduction

The Garba IV *Homo erectus* child from Level E at Melka Kunture (Ethiopia) has been dated to circa 1.5 Ma and assigned to *Homo erectus* based on morphometric analysis of the teeth and mandibular corpus (see Condemi, in this volume). The specimen comprises part of the right side of the mandible of a young child with the empty socket of the right deciduous canine, a much worn first deciduous molar (dm1) and unworn second deciduous molar (dm2; Fig. 1). The lingual surface of the mandibular corpus is broken revealing part of the developing permanent lateral incisor and canine anteriorly, and exposing the first permanent molar (M1) posteriorly (Fig. 1). Enamel of all the teeth in the Garba IV specimen is abnormal with marked wrinkling of the occlusal surfaces of the unworn dm2 and M1 and hypoplastic enamel, including vertical grooves along the sides of the teeth.

As described by Condemi (in this volume), attrition in the dm1 is exceptionally severe for such a young child and the worn occlusal plane slopes markedly in a mesio-distal direction rather than showing the usual horizontal wear plane. Moreover, radiographs indicate that the enamel is hypomineralized (Fig. 2). These features are characteristic of the teeth of children in modern populations suffering from amelogenesis imperfecta, an inherited condition associated with dental defects (Witkop and Sauk 1976).

In order to evaluate the significance of the pathology observed in the Garba IV teeth, we compared the specimen with other fossils as well as with teeth of healthy modern children and children diagnosed with amelogenesis imperfecta. Comparisons were carried out using radiographs, in order to compare the developmental stage of the teeth relative to attrition and to assess the effect of geological age and fossilization on the radio-opacity of internal structures. In addition, the ultra structure of the enamel of the Garba teeth was examined using scanning electron microscopy (SEM).

1. Laboratory of Bio-anthropology and Ancient DNA, Hebrew University, Hadassah Faculty of Dental Medicine, Jerusalem, P.O. Box 12272, Jerusalem; Pedodontic Department, Barzilai Medical Center, Ashkelon, Israel. Tel. 972 2 6757608; fax 972 2 6784010. uri-z@inter.net.il. 2. Laboratory of Bio-anthropology and Ancient DNA, Hebrew University, Hadassah Faculty of Dental Medicine, Jerusalem, P.O. Box 12272, Jerusalem, Israel. Tel. 972 2 6758577; fax 972 2 6784010. pat@cc.huji.ac.il. 3. CNRS UMR 6578, Faculté de Médecine la Timone, 27 rue Jean Moulin, Marseille Cedex 5, F-13385, France. silvana.condemi@voila.fr
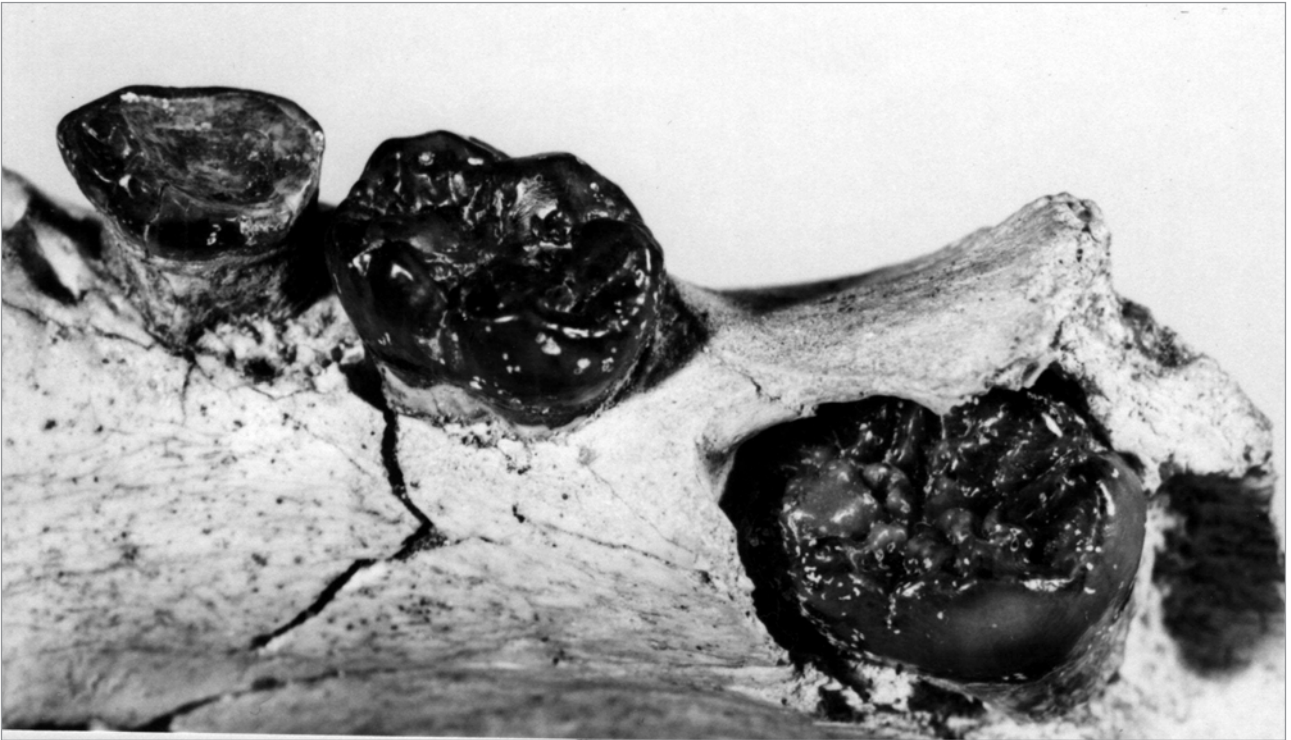
Fig. 1. Garba IV mandible from occluso-lingual view showing the dental developmental stages of M1 and the peculiar pattern of attrition on dm1.

Fig. 2. Radiograph of the Garba IV mandible.

U. Zilberman, P. Smith, S. Condemi

Dental age determination and attrition

The teeth that can be identified on the Garba IV radiograph are: the unerupted first permanent molar (M1) in its crypt with bone covering the occlusal surface and crown completed as well as 1 mm of the root; the erupted second deciduous molar (dm2) with roots almost complete; the erupted first deciduous molar (dm1) with marked attrition on the distal part of the tooth and fully formed roots; the follicles of the first and second permanent premolars and canine with developing crowns.

This stage of dental development corresponds to a chronological age of 2.5-3 years in modern populations (Morrees *et al.* 1963; Stewart *et al.* 1982; Liversidge *et al.* 1999). Figures 3-6 show examples of successive stages of development in modern children aged 2-4 years. Figure 3 shows the developing teeth of a boy aged 2 years and 2 months. The M1 crown is still incomplete and the follicle is covered with bone and the roots of the second deciduous molar are ¾ formed. Figure 4 shows the developing teeth in a slightly older boy (2.5 years). The M1 is complete but is still covered with bone and the roots of the second deciduous molar are fully formed. The first premolar has begun to calcify, and the follicle of the second premolar is clearly defined. Figure 5 shows the developing teeth in a 3 years old girl. Root development in the first permanent molar is well advanced and the second permanent molar has begun to calcify. Figure 6 shows the developing teeth of a girl aged 4 years and 3 months. The M1 has started erupting and root development is well advanced. Calcification of the first premolar crown is almost complete and the second premolar has begun calcifying.

Dental age of the Garba IV child is then most similar to that of the 2.5 year old child using modern standards. However, dental development in early hominids was faster than that of recent humans due to a combination of more rapid enamel extension and faster enamel secretion rates. This applies both to hominids predating the Garba IV specimen, such as the Australopithecines (Beynon and Wood 1987) as well as to the more recent Neanderthals (Dean *et*
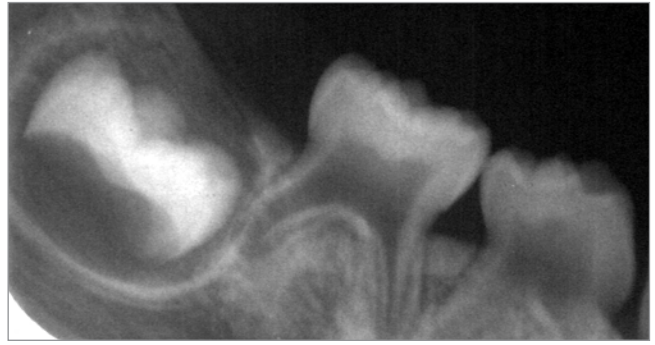
Fig. 3. Bite wing radiograph of a 2 years and 2 months old modern child.

Fig. 4. Bite wing radiograph of a 2 years and 6 months old modern child.

Fig. 5. Bite wing radiograph of a 3 years old modern child.

Fig. 6. Bite wing radiograph of a 4 years and 3 months old modern child.
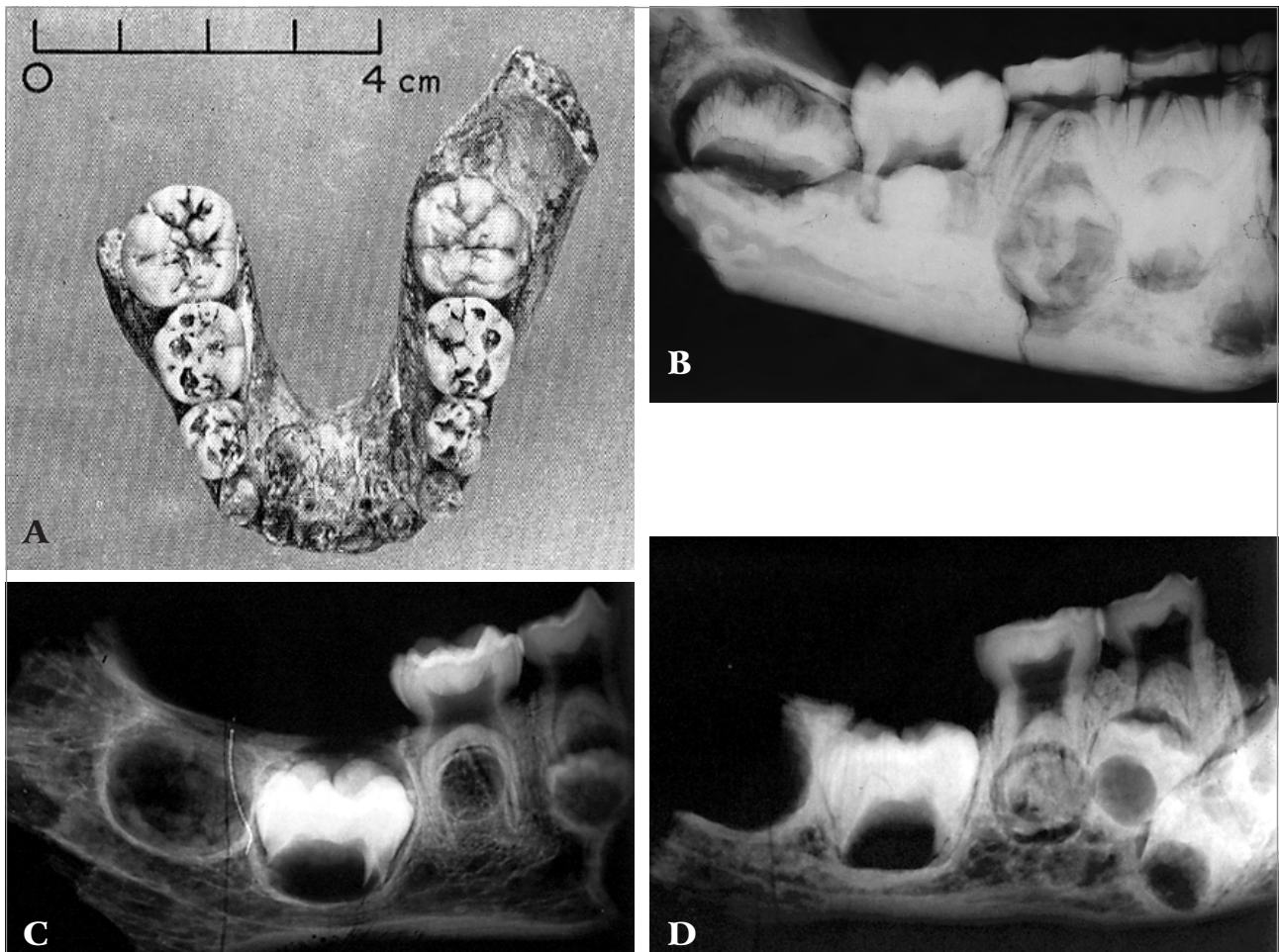
Fig. 7. Fossil hominids: A. Taung mandible, B. radiograph of Sk63 mandible, C. radiograph of Gibraltar II mandible, D. radiograph of La Chaise, abri Suard 13 mandible.

al. 1986; Zilberman and Smith 1992; Skinner 1997; Ramirez Rozzi *et al.* 2004). Thus, the chronological age of fossil children has been estimated as ⅔, ½ of that of modern humans with the same stage of dental development (Bromage and Dean 1985, Dean *et al.* 1993a, b). This suggests a chronological age for the Garba IV child of less than 2 years, so that the dm1 has been in occlusion for only a short time.

Comparison with others fossils children

In order to examine further the significance of the severity and pattern of attrition of the Garba IV specimen, a number of comparisons were made with other fossil children. Since no *Homo erectus* specimens were available for comparison, we compared the Garba IV individual to geologically older and younger fossils. They include two australopithecines (Taung and Sk 63; radiographs supplied by G. Sperber) and two Neanderthals (Gibraltar and La Chaise, radiographs courtesy of M. Skinner).

Both australopithecine specimens show more advanced dental development than the Garba IV child, but significantly less attrition on the deciduous molars. The Taung child (Fig. 7A), has all deciduous teeth present and erupting first permanent molars. Attrition in the deciduous molars is much less pronounced than in Garba IV, despite the more advanced dental age of the Taung child, whose age has been estimated as 3.3 years (range 2.7-3.7) based on a comparison with Sts 24a and upon counts of perikymata (Bromage 1985; Day 1988). This would correspond to an age of 5-6 years based on modern standards. The radiograph of the Sk63 (Fig. 7B) shows more advanced dental development than the Taung child. The M1 are

in occlusion and root formation is well advanced. The crowns of the second permanent molars and first premolars are complete, and crown development of the second premolar is well advanced. Root formation in both deciduous molars is complete and pulp height is reduced due to secondary dentine formation indicating that these teeth have functioned in the mouth for some years. In Sk 63 both deciduous molars show considerable attrition, but the occlusal plane is horizontal indicating gradual and regular wear over the entire occlusal surface. This contrasts to the marked mesio-distal slope of the occlusal surface seen in the much younger Garba IV child, where there is no secondary dentine.

Figures 7C and 7D show radiographs of the Gibraltar II and La Chaise 13 mandibles, accordingly, with dental development similar to that of the Garba IV specimen. In both specimens the dm1 and dm2 are in occlusion, while the crowns of the first permanent molar are complete with 1-2 mm of root formed. As in the Garba IV specimen, there is no secondary dentine formation. The disparity between the severe attrition in the Garba specimen and absence of attrition into dentin in the Neanderthals is pronounced.

In conclusion, the age of death of the Garba IV child was between 2.5 and 3 years compared to modern populations, or 1.6-2 years using standards developed for fossil hominids. The use of developmental stages, for comparison, emphasizes the unique pattern and severity of attrition of the Garba IV teeth. This combined with the surface appearance of the teeth, and lack of definition of enamel on radiographs suggests that the enamel was incompletely mineralized.

Structure of the Garba IV teeth

In the Garba IV mandible (Fig. 1) the dm1 is extensively worn especially on the distal portion. The dm2 and M1 show abnormal occlusal morphology with extensive wrinkling and numerous additional marginal cuspules. The sides of the teeth show numerous hypoplastic lesions, pits and vertical grooves. The radiographic examination of the Garba IV mandible (Fig. 2) shows no distinction between the enamel and dentine, indicating that the enamel was hypomineralized.

Normal mature enamel contains less than 4% of organic matrix. Bone and dentine contain well over 30% organic matrix, thus they are less radio-opaque than the enamel of normal teeth. The difference in the ratio of organic to mineralized components also means that fossilization will affect the opacity of enamel far less than that of bone and dentine. The opacity of the enamel, dentine and bone in the Garba IV specimen is identical to that seen in modern cases of hypocalcified amelogenesis imperfecta (AI), with little differentiation between enamel and dentine but with excellent definition of the internal trabeculae of the bone, tooth roots and pulp cavities. This picture contrasts markedly with that seen in hypermineralized fossil jaws, such as that of the Swartkrans child Sk 55b (Fig. 8), where little internal definition is visible in either the bone or teeth.

Tobias (1986), noted the presence of occlusal wrinkling in Australopithecine molars, and suggested that this might be an expression of hypoplasia. However, the condition as described by him was not associated with the presence of enamel defects elsewhere on the teeth. Linear enamel hypoplasia attributed to developmental stress has been recorded in most living and fossil primates and appears to have been fairly common in australopithecines as well as other early hominids (White 1978;
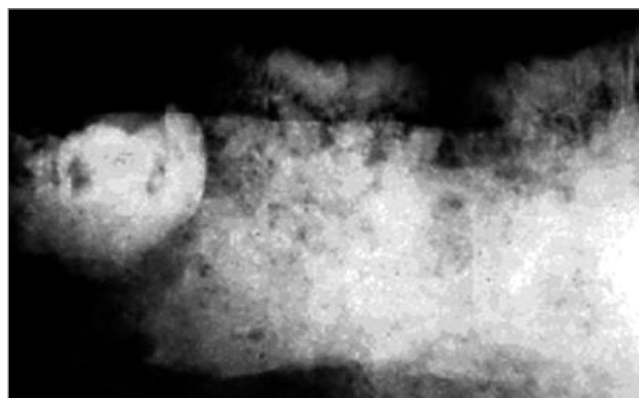

Fig 8. Radiograph of Sk 55b mandible.

Evidence for a genetic disorder affecting tooth formation in the Garba IV child

Brunet *et al.* 2002; Guatelli and Steinberg 2003; Skinner and Newell 2003). It occurs as discrete lesions within otherwise normal enamel and the location of the defects represents the timing of the developmental insult. Since the teeth develop at different times, the location of the defect varies from tooth to tooth. This differs from the condition seen in amelogenesis imperfecta (AI), where all teeth are affected in similar regions because of an inherited defect in enamel formation. The similar degree of mineralization of dentin and enamel in AI also means that enamel rims are smoothed, like dentin, rather than showing the raised enamel rims characteristic of normal enamel. When compared to the modern AI cases, the smooth worn occlusal surface of the first deciduous molar, with poor surface delineation between enamel and dentin, lacking raised enamel rim is similar to that seen on the worn surfaces of the upper incisors seen in hypocalcified AI (Fig. 14). The wrinkled occlusal surfaces of the Garba IV molars also resemble that shown in recent individuals with AI shown in Figs. 15-16.

Amelogenesis imperfecta

Amelogenesis imperfecta (MIM #301200) represents a broad spectrum of genetic diseases affecting enamel formation in both deciduous and permanent dentition. AI has been classified into 14 different subtypes according to the clinical appearance of the enamel and the Mendelian mode of inheritance (Witkop and Sauk 1976; Aldred *et al.* 2003). The prevalence of AI has been reported as 1:14000 in the USA (Witkop and Sauk 1976), 1:8000 in Israel (Chosack *et al.* 1979), 1:4000 in Sweden (Bäckman and Holmgren 1988) and as high as 1:700 in the Vasterbotten county of Sweden (Bäckman and Holm 1986).

The alleles associated with AI include autosomal dominant or recessive and X-linked dominant or recessive (Witkop and Sauk 1976). The X-linked form, AIH1, results from mutations in the X-chromosome amelogenin gene (AMELX). Some 12 allelic mutations have been reported (Hart *et al.* 2002; Hu, Yamakoshi 2003). A second locus for X-linked recessive AI, AIH3, has been mapped to chromosome Xq24-q27.1 (Forsman *et al.* 1994). Mutational analyses and careful evaluation of the phenotype of affected individuals with X-linked type have revealed genotype-phenotype correlations (Hart *et al.* 2000; Ravassipour *et al.* 2000, Li *et al.* 2003; Wright *et al.* 2003). The autosomal-dominant form of AI are the most prevalent forms, representing over 95% of all reported cases and have been shown to be genetically heterogenetic (Bäckman 1997). An autosomal–dominant, local hypoplastic form of AI (AIH2) has been mapped to a 4 Mb region of human chromosome 4q11-q21 that encompasses the gene encoding the ameloblast-specific protein ameloblastin, AMBN (Mardth *et al.* 2001) and the enamelin gene, ENAM (Kida *et al.* 2002). Lately, indentification of a locus on chromosome 2q11 at which recessive AI and cone-rod dystrophy cosegregate has been reported (Downey *et al.* 2002).

The enamel in AI may be characterised as hypocalcified, hypomature or hypoplastic. Distinctive clinical features may be observed in each variant (Witkop and Stewart 1982). However all AI patients suffer from poor aesthetics because of discolouration and severely worn teeth, sensitivity to hot/cold and sweet/sour because of lack of enamel and loss of occlusal vertical dimensions from excessive attrition. The mildest problems are found in the pitted hypoplastic type, whereas the most severe are encountered in the hypocalcified form (Seow and Amaratunge 1988). The mean enamel mineral content is reduced and is associated with an increased protein content (Wright *et al.* 1995). The hypomature form is characterised by an increased praline content, while in hypocalcified AI, enamel has increased tyrosine (Wright *et al.* 1997). Hypocalcified AI may be associated with a disturbance of matrix protein degradation during the maturation phase (Takagi *et al.* 1998). All forms of AI show both hypoplastic and hypomineralized areas under the SEM (Bäckman *et al.* 1989; Bäckman *et al.* 1993). In deciduous teeth, the enamel shows irregu-

larities in enamel crystallites and hypoplastic areas. Seymen and Kiziltan (2002) also reported irregular canaliculi in the predentine, while Sanchez-Quevedo and colleagues (2001) have shown that the prisms in AI teeth are parallel or irregularly decussated with occasional filamentous prisms accompanied by small, irregularly rounded formation. Moreover, calcium levels differ significantly between anterior and posterior teeth. This indicates that the factors influencing normal mineralization in different regions of the dental arch are not altered in the process of AI.

Hypocalcified AI is characterized clinically by yellow-brown colored enamel that is prone to severe attrition, often leading to rapid destruction of the crown. This particular form of AI is associated with decreased mineralization as well as ultrastructural defects in the crystallite structure (Wright *et al.* 1993). The genes responsible for hypocalcified AI have not been identified, although a number of autosomal genes have been proposed as candidates based on their expression by ameloblasts, including ameloblastin and enamelin (chromosome 4q13.3), tuftelin (chromosome 1q21), enamelysin (chromosome 11q22.3-q23) and kalikrein 4 (chromosome 19q13.3-q13.4; Hart *et al.* 2003). The enamel of newly erupted teeth is of normal thickness but very soft. At the cervical part of the crown the enamel is often better calcified than other portions of the crown. The enamel is not uniformly affected in all areas of the teeth with the lingual surfaces of the mandibular central incisors appearing clinically normal. Wright and colleagues (1993) examined teeth affected by hypocalcified AI using light microscopy and SEM. The affected enamel was observed porous under the light microscope. SEM analysis showed the enamel to be prismatic with relatively normal prism morphology but the crystallites were granular. The granular appearance is due to mineral abnormality. The enamel was less radiopaque and poorly mineralized compared to normal enamel. Chemical determination of the mineral per volume showed some areas of the enamel to contain as much as 30% less mineral compared to normal enamel. The carbonate content was similar to normal enamel. Anterior open bite has been recorded in over 60% of the cases observed and the enamel fails to contrast with the dentin radiographically (Witkop and Stewart 1982).

Clinical and radiographic comparison of the Garba IV mandible to AI cases observed in modern children

Case no. 1- Hypoplastic AI- L.O., a 2.5 years old boy (Figs. 9-13). The gross tooth morphology is normal with a moth-eaten appearance and a yellowish discoloration due to very thin enamel. A class II div 1 occlusion can be observed with marked open bite (Fig. 9). The most affected teeth are the upper incisors while the lower incisors show minimal effect. Remnants of the thin enamel can be observed on the buccal aspect of the upper deciduous incisors. The enamel on the deciduous incisors is fractured on the mesial and distal surfaces. The deciduous molars show no attrition (Figs. 10, 11). On the bite-wing radiographs the very thin enamel can be observed on the deciduous molars and permanent molars (Figs. 12, 13). The morphology of the pulp chambers is normal.

Case no. 2- Hypocalcified AI- E.S., a 3 years old girl (Figs. 14-18). The upper incisors show severe attrition and brown discoloration. The upper incisors are the most affected while the lower incisors show normal morphology and light brownish discoloration (Fig. 14). The first deciduous molars show attrition and missing enamel while the second deciduous molars show altered morphology with regions of missing enamel on both upper and lower jaws (Figs. 15, 16). On the bite-wing radiographs no distinction can be observed between enamel and dentin on deciduous molars or on the developing first permanent molars (Figs. 17, 18).

Fig 9. Front view of a 2 years 6 months old boy (L.O.) suffering from hypoplastic amelogenesis imperfecta.
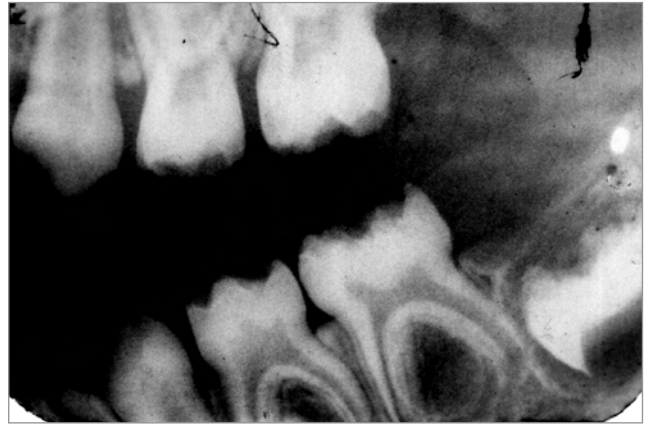

Fig. 13. Left bite-wing of L.O.
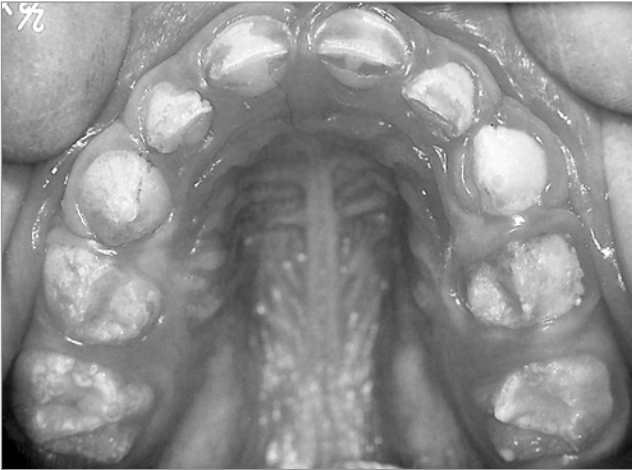
Fig. 10. Upper jaw of L.O.- occlusal view.

Fig. 14. Front view of a 3 years old girl E.S., suffering from hypocalcified amelogenesis imperfecta.
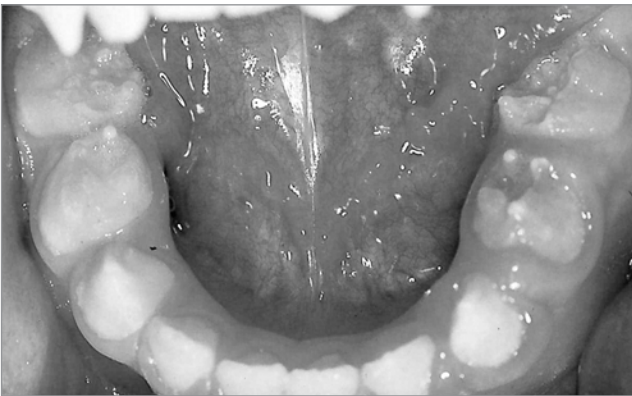

Fig. 11. Lower jaw of L.O.- occlusal view.

Fig. 15. Upper jaw of E.S.- occlusal view.

Fig. 12. Right bite wing of L.O.

Fig. 16. Lower jaw of E.S.- occlusal view.

U. Zilberman, P. Smith, S. Condemi

Fig. 17. Right bite-wing of E.S.
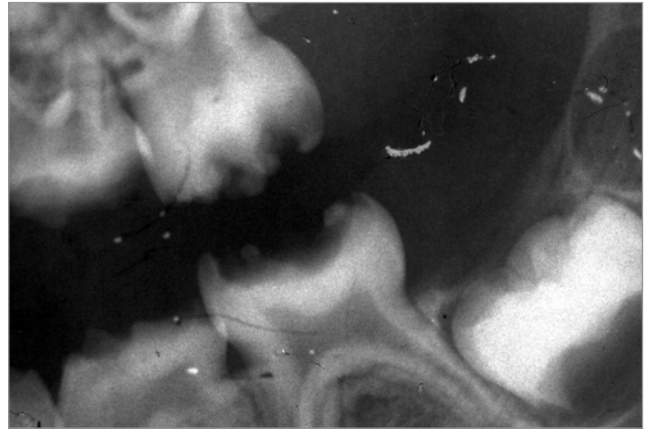
Fig. 18. Left bite-wing of E.S.

SEM analysis of the Garba IV mandible

Epoxy resin casts were made from silicone impressions of the Garba IV teeth. To minimize air bubbles the silicone impression was placed in a vacuum chamber together with a fresh mixture of low viscosity epoxy resin for five minutes and then filled with the resin and returned to the vacuum chamber for an additional five minutes. The epoxy was left overnight at room temperature to harden and then peeled away from the silicone impression. The casts were coated with colloidal gold and examined under a scanning electron microscope at magnifications ranging from x30-x2000, and compared with a normal exfoliated deciduous tooth with attrition into dentin.


Occluso-Buccal view

x150

Hypoplastic region - x50
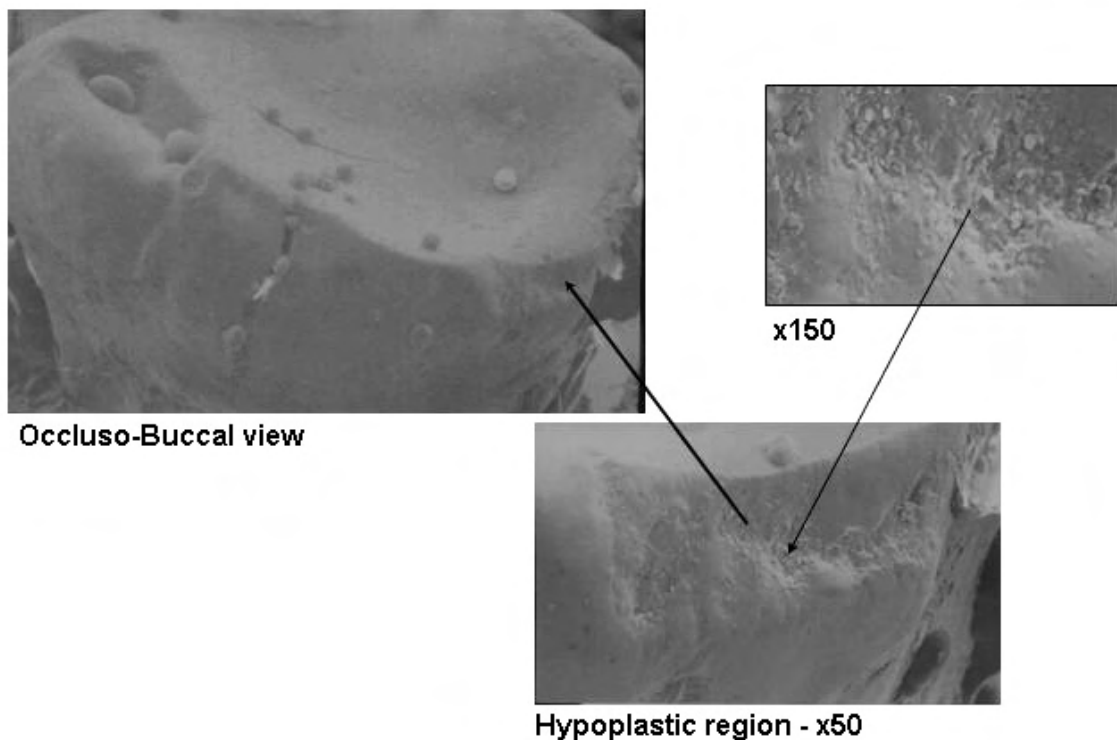
Fig. 19. SEM picture of dm1 of Garba IV mandible.

Evidence for a genetic disorder affecting tooth formation in the Garba IV child
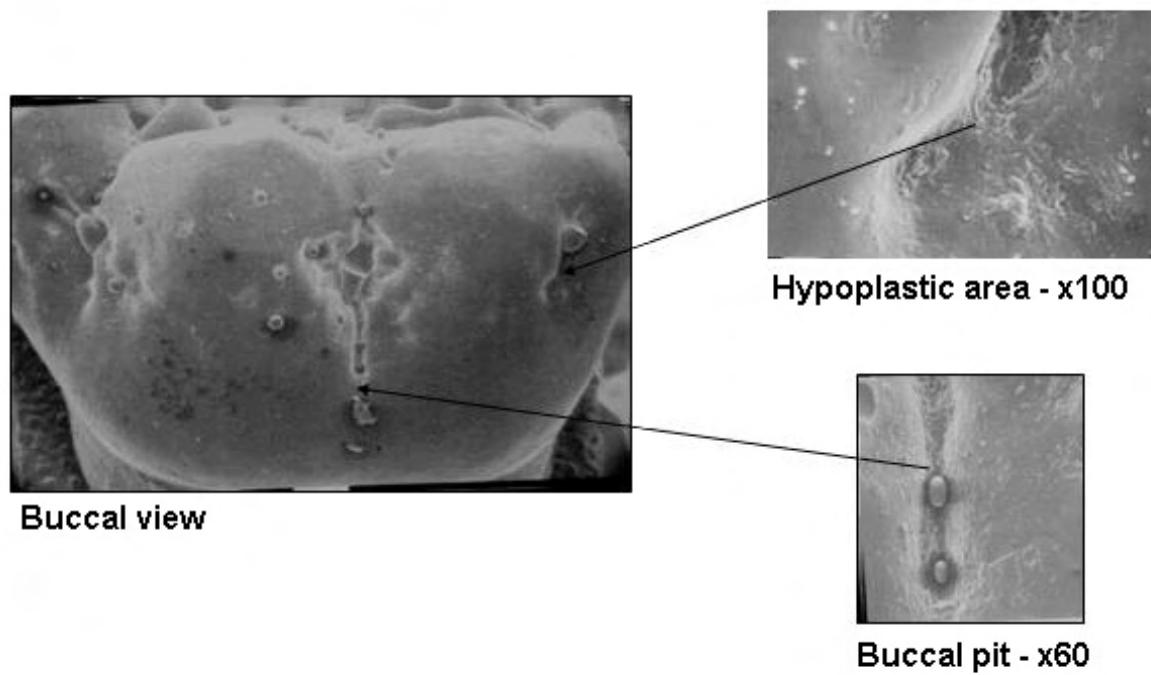
Fig. 20. SEM picture of dm2 of Garba IV mandible.
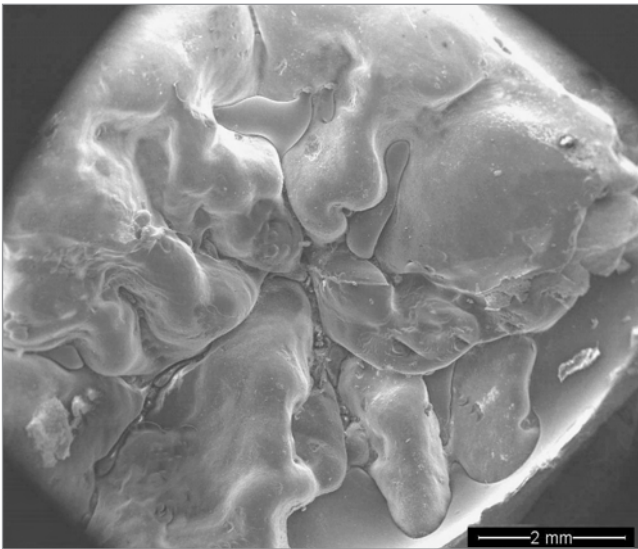
Fig. 21. SEM picture of M1 of Garba IV mandible.

Figures 19 and 20 show SEM pictures of dm1 and dm2. The first deciduous molar shows extensive wear with regions of missing enamel and hypoplastic areas on the buccal surface. The second deciduous molar shows areas of hypoplastic enamel and poor coalescence of cusps as observed on buccal fissures and pits. The occlusal surface of the first permanent molar (Fig. 21) is excessively wrinkled, with numerous small cuspules. The unworn surfaces of the dm2 and M1 are excessively wrinkled, with numerous small cuspules especially on the occlusal margin, while the buccal fissures are deep and lack enamel at their bases. At high magnification the enamel surface shows a mosaic appearance with numerous shallow pits (Figs. 20, 21) identical to those reported in modern patients with AI. The abraded occlusal surface of Garba IV dm1 lacks the well defined enamel rim seen in normal teeth and enamel and dentin show a similar smooth surface (Fig. 22). The abraded occlusal surface of Garba IV dm1 lacks the well defined enamel rim with sharp edges at the enamel-dentin margin seen in the normal tooth (Fig. 22B, D) and enamel and dentin show a similar smooth surface (Fig. 22A, C). Taken in conjunction with the reduced enamel radio-opacity and severe attrition, the findings are indicative of amelogenesis imperfecta.
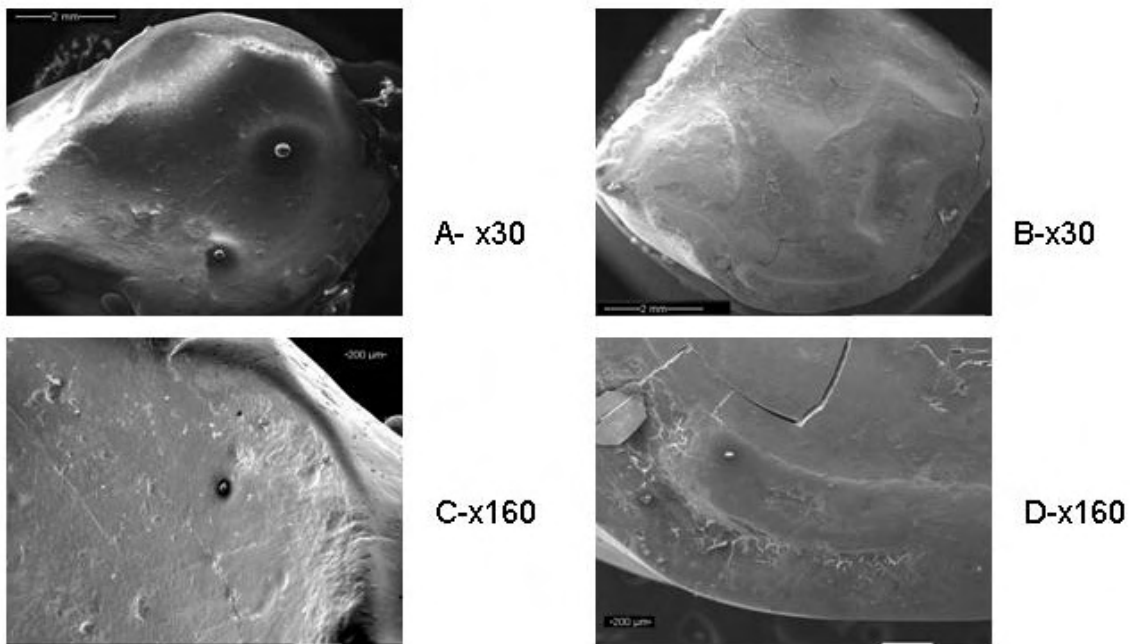
Fig. 22. SEM picture of dm1: A. Occlusal surface of Garba IV x30. B. Occlusal surface of healthy modern child x160. C. Occlusal surface of Garba IV x30. D. Occlusal surface of healthy modern child x160.

Conclusions

We propose that the anomalies of the enamel surface, combined with the reduced radio-opacity, severe attrition, location and type of hypoplastic defects seen on the SEM images indicate that the Garba IV child is an early example of AI. While AI is not in itself a fatal disease, the rapid attrition of teeth, discomfort of chewing and consequent lack of ability to deal with even a soft diet that is characteristic of the condition, must have been a serious handicap to survival in the past. Since skeletal remains of young children are relatively rare, it is not surprising that little evidence of this condition has been found in early hominids, even though the numerous mutations associated with AI suggests a long evolutionary history.

This study provides evidence of a direct genetic link between *Homo erectus* and modern humans. It enables us to test some of the models for mutation rates that have been put forward by molecular biologists and substantiates modern genetic studies that indicate a long evolutionary history for amelogenesis imperfecta.